Magnetic structure of $GdCu_6$

2009 J. Phys.: Condens. Matter 21 126002

(http://iopscience.iop.org/0953-8984/21/12/126002)

J. Phys.: Condens. Matter **21** (2009) 126002 (6pp) doi:10.1088/0953-8984/21/12/126002

Magnetic structure of $GdCu_6$

Anton Devishvili[1,2], Martin Rotter[2,3], Mathias Doerr[4], Brigitte Beuneu[5] and Günter Behr[6]

[1] Institut Laue Langevin, Grenoble, France
[2] Institut für Physikalische Chemie, Universität Wien, Austria
[3] Department of Physics, University of Oxford, Clarendon Laboratory, Oxford, UK
[4] Institut für Festkörperphysik, TU Dresden, Germany
[5] Labaratoire Leon Brillouin, CEA-CNRS, Saclay, France
[6] Institut für Festkörper und Werkstoffforschung, Dresden, Germany

Received 2 October 2008, in final form 4 February 2009
Published 3 March 2009
Online at stacks.iop.org/JPhysCM/21/126002

Abstract
Hot neutron diffraction has been used to study the magnetic structure of $GdCu_6$. Long range antiferromagnetic order with a propagation vector of (h 0 0) has been determined below the Néel temperature $T_N = 16$ K from the neutron powder refinement. The magnetic moments are oriented normal to the a direction, which is in agreement with previously reported results of bulk experiments. Mean field model calculations suggest that the magnetic structure is a helix.

(Some figures in this article are in colour only in the electronic version)

1. Introduction

The Gd^{3+} based rare earth systems are of particular interest due to the largest spin in the periodic table. The 4f shell is half filled with spherically symmetric charge density and has no orbital moment ($L = 0$). Thus they represent initial model systems for the study of spin–spin interactions. There are no first order crystal field effects present in this type of system. In other rare earth systems the crystal field is claimed to be responsible for magnetic anisotropy [1–3]. However, large anisotropy has been found in a number of Gd compounds [4] and the source of this anisotropy is still under discussion [5–7].

$GdCu_6$ is an orthorhombic system with spacegroup $Pnma$. Thermal variations of susceptibility along different directions in the paramagnetic state show significant anisotropy. Paramagnetic Curie temperatures have been determined to be −32.1 K, −30 K and −2.61 K along a-, b- and c-axes, respectively. Susceptibility and magnetization at low temperature indicate an antiferromagnetic order below the Néel temperature $T_N = 16$ K [8]. The temperature dependence of the specific heat shows an additional transition at $T_r = 15.8$ K. The estimated effective magnetic moment per Gd^{3+} ion is $\approx 7.8\mu_B$ [9]. The saturation field $\mu_0 H_s \approx 24$ T was deduced from magnetization in pulsed high magnetic field [9].

2. Sample preparation

The polycrystalline GdCu6 sample was prepared at IFW, Dresden by a levitation melting technique from pure gadolinium with purity of 99.9% and copper with purity of 99.999%. A Hukin type cold crucible with argon atmosphere was used for this alloying. To ensure homogeneity of the reacted components the resulting droplets were annealed at $T = 800\,^{\circ}$C for 72 h. The purity of the resulting sample has been verified by x-ray powder diffraction.

3. Neutron diffraction

Due to the high neutron absorption cross-section of natural Gd for thermal neutrons, the magnetic structure was studied by hot neutrons. The powder diffraction patterns were collected at the 7C2 instrument at LLB, Saclay. A neutron wavelength of 0.57 Å was selected by a Ge(311) monochromator.

The resulting amount of powder measured was about 8 g. In order to reduce absorption, the powder was placed in a vanadium annular sample holder. Two diffraction pattern were collected at temperatures of 2 and 30 K with a counting time of 9 h. An empirical background I_{bkg} was estimated from the neutron diffraction pattern of a fully absorbing (cadmium foil) sample I_{cd} and an empty sample holder I_{empty} using the following formula: $I_{bkg} = I_{cd} + k(I_{empty} - I_{cd})$ where $k = 0.3807$.

Because of the resonance effects in natural Gd the neutron scattering cross-section is wavelength dependent. For the neutron energies of about 0.25 eV the effective coherent cross-section of 10.2 fm (with real part of 9.99 and −0.82 fm as the imaginary part) was used [10]. The FullProf package was used to analyze the diffraction pattern.

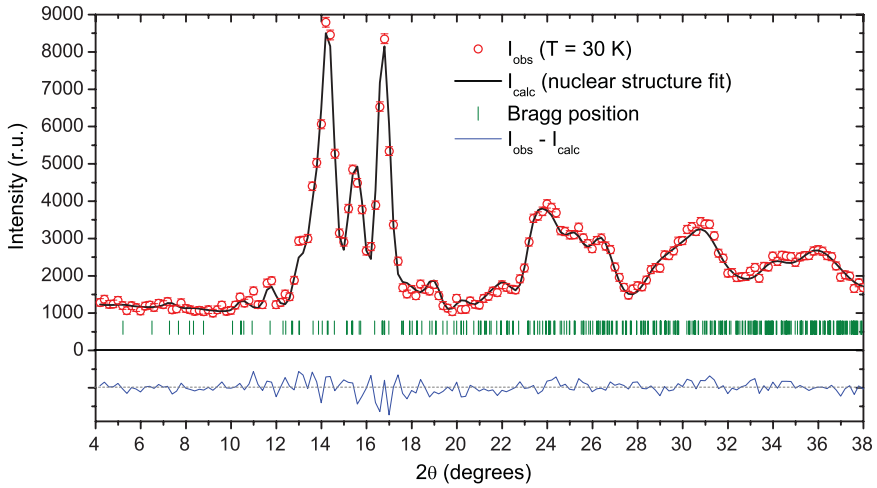

Figure 1. Hot neutron diffraction data obtained at 7C2, Saclay. Red open circles represent experimental data measured above the ordering temperature. The line represents the Rietveld refinement of the nuclear structure.

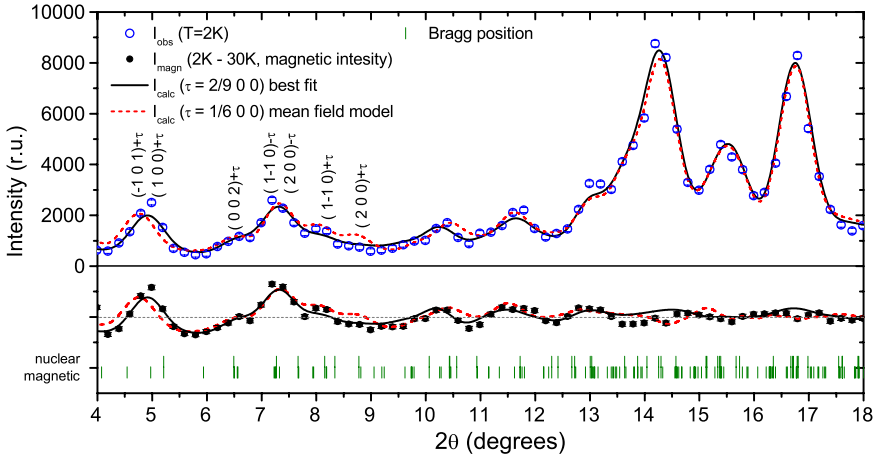

Figure 2. $GdCu_6$ hot neutron diffraction data obtained at 7C2, Saclay. Blue open circles represent experimental data measured below the ordering temperature. The line represents the fit of magnetic and nuclear structures. Black dots below represent the difference between the high and low temperature diffraction pattern.

Table 1. Results of refinement of atomic positions with the Rietveld method.

Atom	Wyckoff index	x	y	z	Temperature factor (Å^2)
Gd	4c	0.257(9)	0.250	0.566(9)	0.1(2)
Cu1	8d	0.050(9)	0.477(9)	0.313(9)	0.2(2)
Cu2	4c	0.060(9)	0.250	0.077(9)	0.3(2)
Cu3	4c	0.142(9)	0.250	0.853(9)	0.3(2)
Cu4	4c	0.292(9)	0.250	0.272(9)	0.3(2)
Cu5	4c	0.375(9)	0.250	0.005(9)	0.3(2)

The nuclear structure was fitted to the 30 K powder pattern. Results of the Rietveld refinement are summarized in table 1 and presented in figure 1. Unit cell dimensions were determined to be $a = 0.8023$ nm, $b = 0.5027$ nm, $c = 1.0075$ nm.

Neutron diffraction data at low temperature clearly indicate the presence of a long period possibly incommensurate structure. A scripting interface was written for the FullProf package in order to resolve the magnetic structure. Different antiferromagnetic configurations were sequentially introduced to the FullProf program to calculate the diffraction pattern. The simulated configurations are all those commonly observed in rare earth antiferromagnets and include collinear structures, amplitude modulated structures as well as a set of cycloids with moments aligned along different directions. The maximum size of the magnetic structure supercell was $10 \times 10 \times 10$ nuclear unit cells. The results of the low temperature neutron powder diffraction fit are presented in figure 2.

The magnetic propagation vector $\tau = (2/9\ 0\ 0) \approx (0.22\ 0\ 0)$ has been determined from the diffraction pattern (figure 2). Several different antiferromagnetic configurations with this propagation vector have been calculated in order to match the magnetic intensity. The magnetic moments restricted to the bc-plane reproduce the measured scattering intensity. Within the experimental resolution, assuming an equal moment collinear structure in the bc-plane, the moment

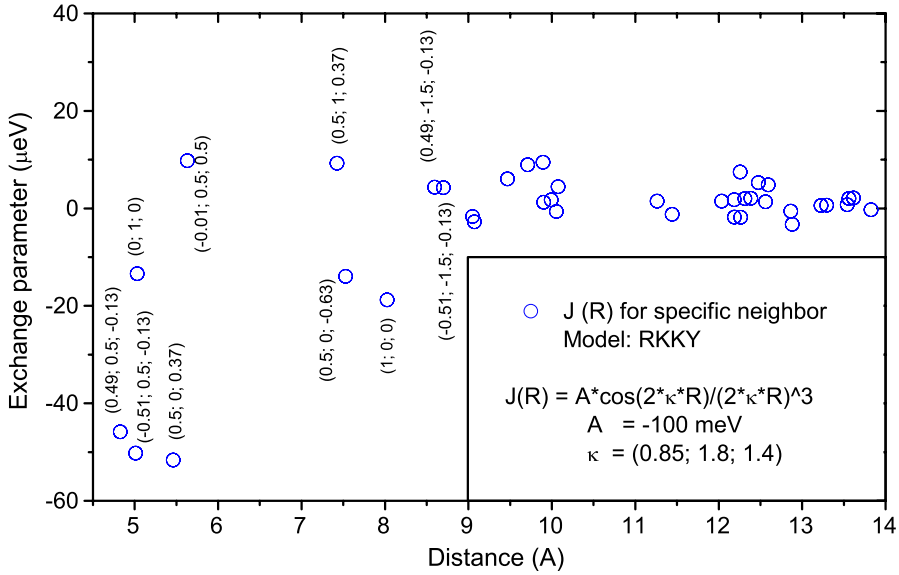

Figure 3. RKKY exchange parameters calculated using equation (7). Dots represent the exchange constants $\mathcal{J}(R)$ where R is the distance to equivalent neighbors.

direction along the [021] direction, e.g. ≈45° between b and c, was refined. Such a magnetic configuration gives same scattering intensities as a helical structure with equal moments.

4. Simulation

In a 4f Gd^{3+} system without single ion anisotropy the magnetic Hamiltonian is a sum of the isotropic exchange ($\mathcal{J}_{\alpha\beta}(ij) = \mathcal{J}(ij)\delta_{\alpha\beta}$), the classical dipolar ($D_{ij}^{\alpha\beta}$) and the Zeeman interactions:

$$\mathcal{H} = -\tfrac{1}{2}\sum_{\alpha\beta}^{i,j} J_i^\alpha \mathcal{J}_{\alpha\beta}(ij) J_j^\beta - \tfrac{1}{2}\sum_{ij\alpha\beta}(g_J\mu_B)^2 D_{ij}^{\alpha\beta} J_i^\alpha J_j^\beta - \sum_i g_{J_i}\mu_B J_i^\alpha H_\alpha. \quad (1)$$

Here $J_i^{\alpha=1,2,3}$ denote the components of the negative of the angular momentum operator of the ith Gd^{3+} ion, $g_J = 2$ the Landé factor and μ_B the Bohr magneton.

Due to the small magnitude of the classical dipolar interaction $D_{ij}^{\alpha\beta} J_i^\alpha J_j^\beta$ the antiferromagnetic propagation vector is dominated by the spin–spin exchange $\mathcal{J}_{\alpha\beta}(ij) = \mathcal{J}(ij)\delta_{\alpha\beta}$, where $\delta_{\alpha\beta}$ denotes the Kronecker symbol. In order to minimize the free energy, the Fourier transform

$$\mathcal{J}_{\alpha\beta}(Q) = \sum_j \mathcal{J}_{\alpha\beta}(ij) e^{-iQ(R_i - R_j)} \quad (2)$$

will have a maximum at the propagation vector of the antiferromagnetic structure [1]. The magnitude of this maximum can be related to the Néel temperature $T_N = 16$ K (assuming isotropic exchange) in the following way:

$$T_N = \frac{\mathcal{J}(\tau)J(J+1)}{3k_B}. \quad (3)$$

Here $J = \frac{7}{2}$ the angular momentum quantum number of the Gd^{3+} ion and k_B is Boltzmann's constant.

According to [9] $GdCu_6$ shows Curie–Weiss behavior in the paramagnetic state. The inverse susceptibility can be fitted yielding the paramagnetic Curie temperatures $\theta_{\alpha=a,b,c}$ (in our case $\theta_a = -32.1$, $\theta_b = -30$ and $\theta_c = -2.61$ K) along different crystallographic directions. The fact that $\theta_a \approx \theta_b \neq \theta_c$ indicates some significant anisotropy in the two ion interaction $\mathcal{J}_{\alpha\alpha}(ij)$. The Curie temperatures are related within the mean field theory to the magnitude of the Fourier transformation of exchange at $Q = 0$ i.e. $\mathcal{J}_{\alpha\alpha}(Q = 0)$:

$$\theta_\alpha = \frac{\mathcal{J}_{\alpha\alpha}(Q=0)J(J+1)}{3k_B}. \quad (4)$$

Using equations (3) and (4) one can estimate the magnitude of $\mathcal{J}(Q = \tau) \approx 262$ μeV, $\mathcal{J}_{aa}(Q = 0) \approx -527$ μeV, $\mathcal{J}_{bb}(Q = 0) \approx -509$ μeV and $\mathcal{J}_{cc}(Q = 0) \approx -48$ μeV. For a periodic antiferromagnetic structure the critical (saturation) field along different directions is estimated by [1]:

$$H_s^\alpha = \frac{J(\mathcal{J}(\tau) - \mathcal{J}_{\alpha\alpha}(0))}{g_J\mu_B}. \quad (5)$$

Using equations (4) and (3) in (5), the expression for critical field value follows

$$H_s^\alpha = \frac{3k_B(T_N - \theta_\alpha)}{g_J\mu_B}. \quad (6)$$

Using the experimentally obtained values of T_N and θ_α in (6) saturation field along the c direction $\mu_0 H_{sc}^{calc} \approx 9.2$ T is calculated. As seen from the experiment, this value does not correspond to an experimentally measured saturation field $\mu_0 H_{sc}^{exp} \approx 24$ T. However, the calculated saturation fields along a and b show more reasonable values $\mu_0 H_{sa}^{calc} \approx 23.82$ T and $\mu_0 H_{sb}^{calc} \approx 23.28$ T.

We note that due to the fact that there is more than one Gd atom in the primitive crystallographic cell of $GdCu_6$, the above evaluation is not straightforward. The method described

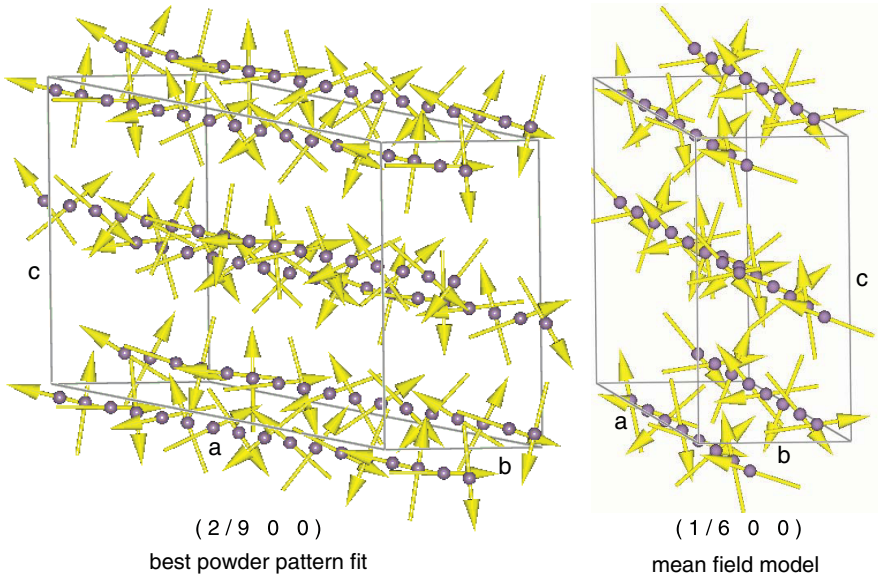

Figure 4. (a) (Left) magnetic structure of $GdCu_6$ at $T = 2$ K fitted from neutron powder diffraction. (b) (Right) calculated magnetic structure of $GdCu_6$ at $T = 2$ K using the mean field model discussed in the text. Only gadolinium atoms are shown.

in [6, 11] cannot be applied directly since expression (2) is valid strictly for a single atom basis. In the case of multiple atoms (n_b) in the primitive unit cell, $\mathcal{J}^{r,s}_{\alpha\beta}(Q)$ in expression (2) has to be expressed as a tensor; the indices $r, s = (1, \ldots, n_b)$ are necessary to express the exchange between different atoms r and s in the primitive unit cell. The diagonalization of this tensor will be required to obtain the Néel temperature for such a system. Although equations (2)–(5) have to be modified accordingly, the resulting expression (6) will remain valid.

In order to simulate the magnetic properties of $GdCu_6$, in a first step the anisotropy seen in the paramagnetic Curie temperature was neglected. Direct exchange effects can probably be neglected in comparison to the RKKY interaction due to the metallic character of this system and the large Gd–Gd distances; the nearest neighbor distance 0.48 nm is large compared to the atomic radius of Gd (0.18 nm). Therefore the spin–spin exchange was chosen to be isotropic and assumed to be oscillating according to the RKKY model [1], generalized to an anisotropic Fermi-surface:

$$\mathcal{J}(r) = A\cos(2\kappa)/(2\kappa)^3 \tag{7}$$

with

$$\kappa^2 = k_a^2 r_a^2 + k_b^2 r_b^2 + k_c^2 r_c^2. \tag{8}$$

The calculation which is described below in detail was performed for different values of the Fermi-surface tensor $k_F = (k_a, k_b, k_c)$ and best correspondence to the experimental propagation vector and other magnetic properties was found for $k_F = (0.85, 1.8125, 1.4)$ Å^{-1}. In order to get the correct magnitude of the Néel temperature the scaling factor A was set to $A = -100$ meV. The parameters are shown in figure 3. In this parameter set the $T_N^{calc} = 17.4$ K and isotropic paramagnetic Curie temperature $\theta_\alpha = -9$ K is in between the experimental values $\theta_a = -32.1$ K and $\theta_c = -2.61$ K.

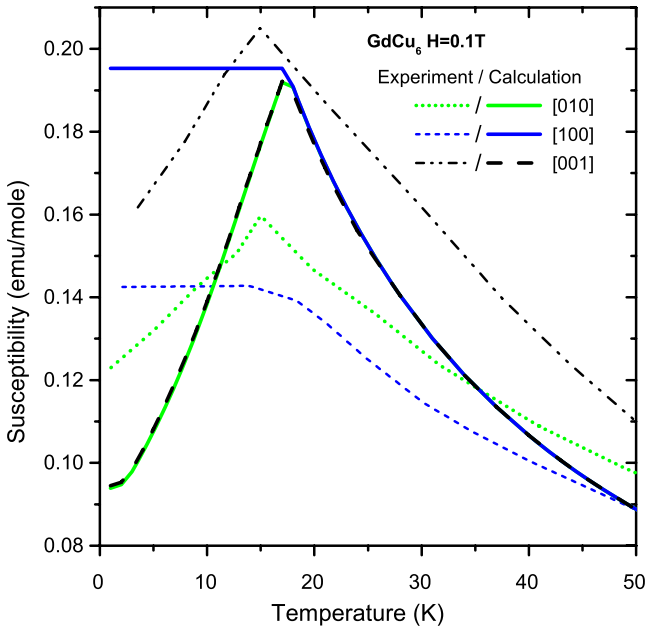

Figure 5. Temperature dependence of magnetic susceptibility along three main crystallographic directions in the low temperature region. Data (dashed lines) were taken from [9]. Calculated magnetic susceptibility is presented as solid lines.

Applying equation (5), the calculated saturation field $\mu_0 H_s^{calc} \approx 14$ T.

Using the *McPhase* modeling suite [12] simulations can be performed within the mean field approximation [1]. In addition to the RKKY interaction $\mathcal{J}(R)$ as parametrized by equation (7) we used the dipolar interaction

$$D_{ij}^{\alpha\beta} = \frac{3(R_i^\alpha - R_j^\alpha)(R_i^\beta - R_j^\beta) - \delta_{\alpha\beta}|R_i - R_j|^2}{|R_i - R_j|^5}. \tag{9}$$

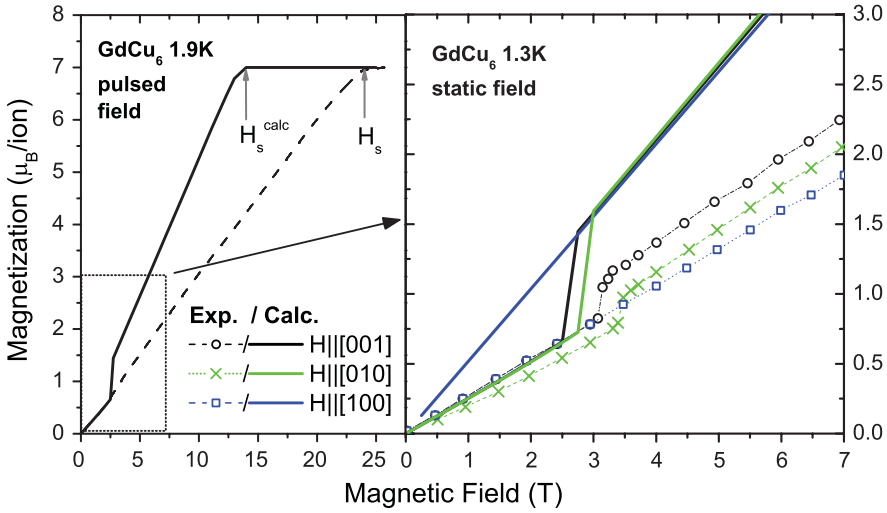

Figure 6. Experimentally measured magnetization of $GdCu_6$ in static and pulsed magnetic field. The magnetic field pulse was applied along the [001] direction. Static magnetic field up to 14 T was used to obtain magnetization for the main crystallographic directions. Data taken from [9] (dashed lines) is compared with results of numerical simulation (bold lines) described in section 5.

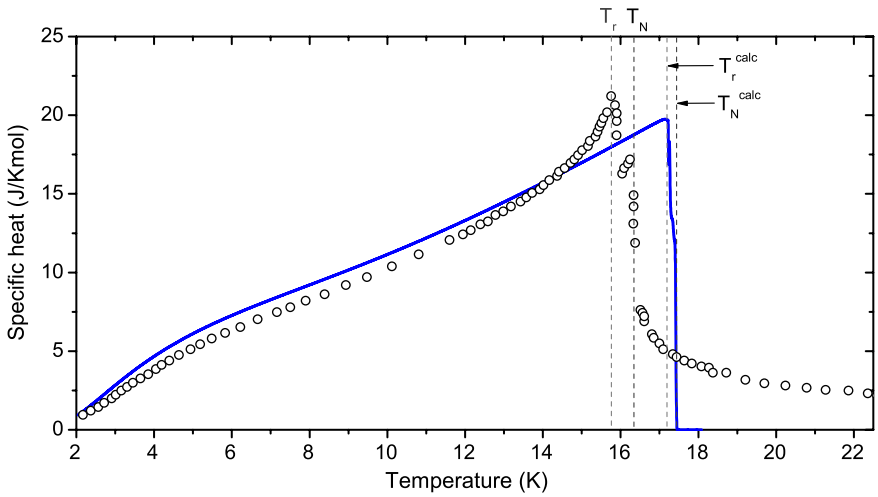

Figure 7. Temperature dependence of magnetic contributions to the specific heat. The data (black open circles) were obtained by subtracting the specific heat of $LaCu_6$ (non-magnetic analog) from that of $GdCu_6$ (e.g. $C_m = C_{GdCu_6} - C_{LaCu_6}$). Data taken from [9]. The solid blue line represents the calculated magnetic contribution to specific heat by the mean field approximation described in section 4.

Details on numerical method can be found in [5, 12] and in the *McPhase* manual[7].

5. Discussion

Treating these interactions in the form of the Hamiltonian (1), a helical magnetic structure was obtained at 2 K with propagation vector $\tau = (0.167\ 0\ 0)$ and moments in the *bc*-plane. Note that the structure is a helix with a turning angle of 60°. Taking into account the considerable experimental error involved in a short wavelength experiment, this is in good accordance with the experimental data. The calculated magnetic structure is shown in figure 4(b).

The diffraction pattern was calculated for this helix and is compared to the experimentally observed pattern in figure 2. Within the experimental resolution the overall agreement is reasonable.

In addition to the magnetic structure at 2 K the temperature dependence of the magnetic susceptibility was calculated and is shown in comparison to experimental data in figure 5. As reported by low temperature susceptibility measurements, the antiferromagnetic hard axis is parallel to the [100] direction, suggesting the *bc*-plane to be an easy plane. As suggested by neutron diffraction experiments and numerical simulations, the magnetic moments are situated in the *bc* plane, thus fully corresponding to an expectation from bulk measurements.

The magnetic contribution to the specific heat can be compared to experimental data in figure 7. From the experimental data and the simulation it can be seen that another antiferromagnetic phase is stabilized in the vicinity of the Néel temperature. According to the calculation in this phase, the

[7] www.mcphase.de

propagation vector stays the same as at lower temperatures (0.167 0 0). However, the moments are aligned in an amplitude modulated collinear structure parallel to the *b*-direction. As in many other Gd compounds such a collinear phase in a narrow temperature range below the Néel temperature may be stabilized by the dipolar anisotropy [4].

The magnetization for magnetic field along the main crystallographic directions has been calculated and is compared with experimental data in figure 6. All main features of magnetization are reproduced but the calculated saturation field $\mu_0 H_s^{\mathrm{calc}} \approx 14$ T while experiment suggests $\mu_0 H_s^{\mathrm{exp}} \approx 24$ T. Such a difference, however, is attributed to the particular values of $\mathcal{J}(r)$ which were fitted to obey $\theta = -9$ K, leading to a too small value of $H_{s\alpha}^{c}$ via relation (5).

6. Conclusion

Since $GdCu_6$ has more than one Gd^{3+} ion in the unit cell, the procedure to obtain the values of $\mathcal{J}(r)$ involves fine tuning a large number of exchange parameters for different symmetrically equivalent neighbors in order to fulfil the maximum of equation (2) at $Q = \tau$ where τ is the experimentally determined propagation vector. To express an exchange within four Gd^{3+} ions in the primitive unit cell twelve independent exchange constants are required. To obtain a long range antiferromagnetic order even more parameters have to be considered. In order to reduce the number of fit parameters a more general formalism of an RKKY exchange (7) is used. Within the particular choice of four parameters in equation (7) exchange between any neighboring atoms can be analytically expressed. To obtain a stable antiferromagnetic configuration the energy of the Hamiltonian (1) has been iteratively minimized. Such formulation of the exchange interaction does not allow us to introduce anisotropy in the paramagnetic region, which is observed in the experimental susceptibility above the Néel temperature. Such anisotropy is expected to lead to a larger difference between T_N and T_r. It can also affect the slope of the magnetization curves along different directions but no other features are expected.

Most of the experimentally observed magnetic features have been reproduced by calculations. The magnetic structure observed by neutron scattering is in agreement with expectations from the dipolar model [4]. However, by comparing the results of our model analysis with the published single crystal bulk magnetization and susceptibility data, we infer that some source of anisotropy other than the dipolar interaction must be present in $GdCu_6$. Additional studies should involve a high resolution magnetic x-ray or neutron diffraction experiment on single crystals.

Acknowledgments

We wish to acknowledge the support of the Austrian Science Foundation (FWF) project P16778-N02 and the French-Austria Bilateral Scientific Technical Exchange Program 'Amadee' project 17/2003. We are grateful to A Hiess for numerous helpful discussion and to P Ambroise for the assistance at LLB, Saclay.

References

[1] Jensen J and Mackintosh A R 1991 *Rare Earth Magnetism* (Oxford: Clarendon)
[2] Rotter M, Loewenhaupt M, Kramp S, Reif T, Pyka N M, Schmidt W and Kamp R V D 2000 Anisotropic magnetic exchange in orthorhombic RCu_2 compounds (R = rare earth) *Eur. Phys. J.* B **14** 29
[3] Loewenhaupt M, Rotter M and Kramp S 2000 Magnetic anisotropies of rare-earth compounds *Physica* B **276–278** 602
[4] Rotter M, Loewenhaupt M, Doerr M, Lindbaum A, Sassik H, Ziebeck K and Beuneu B 2003 Dipole interaction and magnetic anisotropy in gadolinium compounds *Phys. Rev.* B **68** 144418
[5] Rotter M, Schneidewind A, Doerr M, Loewenhaupt M, El Massalami A M and Detlefs C 2004 Interpreting magnetic x-ray scattering of Gd-compounds using the McPhase simulation program *Physica* B **345** 231
[6] Rotter M, Loewenhaupt M, Doerr M, Lindbaum A and Michor H 2001 Noncollinear amplitude modulated magnetic order in Gd compounds *Phys. Rev.* B **64** 014402
[7] Lindbaum A, Gratz E and Rotter M 1994 Anisotropic thermal expansion in $RECu_2$-compounds *Mater. Sci. Forum* **166–169** 467
[8] Roy S B, Lees M R, Stewart G R and Coles B R 1991 Thermodynamic and transport properties of $(Ce_xGd_{1-x})Cu_6$ for $0 \leqslant x \leqslant 1$ *Phys. Rev.* B **43** 8264
[9] Takayanagi S, Ōnuki Y, Ina K, Komatsubara T, Wada N, Watanabe T, Sakakibara T and Goto T 1989 Magnetic properties of antiferromagnetic $GdCu_6$ *J. Phys. Soc. Japan* **58** 1031
[10] Lynn J E and Seeger P A 1990 Resonance effects in neutron scattering lengths of rare-earth nuclides *At. Data Nucl. Data Tables* **44** 191
[11] Blanco J A, Gignoux D and Schmitt D 1991 Specific heat in Gd compounds II. Theoretical model *Phys. Rev.* B **43** 13145
[12] Rotter M 2004 Using McPhase to calculate magnetic phase diagrams of rare earth compounds *J. Magn. Magn. Mater.* **272–276** 481